Electron Spin Resonance of Ni(I) in Ni−Containing MCM-41 Molecular Sieves

Zhixiang Chang, Zhidong Zhu, and Larry Kevan*

Department of Chemistry, University of Houston, Houston, Texas 77204-5641

Received: March 26, 1999

Nickel-containing MCM-41 molecular sieves have been synthesized hydrothermally using cetyltrimethylammonium chloride as a template. The stabilization of Ni(I) in NiMCM-41 is minimal. The various Ni(I) species formed by reduction and adsorbate interactions in NiAlMCM-41 in which Ni(II) is incorporated into a framework position by addition of Ni(II) into the synthesis mixture and in Ni-AlMCM-41 where Ni(II) is incorporated into extraframework positions by liquid state ion exchange were studied by electron spin resonance (ESR) and electron spin−echo modulation. Dehydration at elevated temperature or thermal reduction by hydrogen produces Ni(I) species in Ni-AlMCM-41 which are detectable by ESR. By contrast, in NiAlMCM-41 neither dehydration at high temperature nor hydrogen reduction is effective in producing Ni(I). Ni(I) is obtained in NiAlMCM-41 by γ-irradiation at 77 K. Both NiAlMCM-41 and Ni-AlMCM-41 show differences in their ESR characteristics after reduction and adsorption of D_2O, CO, and ethylene. D_2O adsorption forms $Ni(I)-(O_2)_n$ indicating water decomposition in both materials. CO adsorption onto Ni-AlMCM-41 and NiAlMCM-41 produces $Ni(I)-(CO)_3$ and $Ni(I)-(CO)_2$, respectively. The interaction between Ni(I) and ethylene seems weaker in NiAlMCM-41 than in Ni-AlMCM-41. The contrasting characteristics of Ni(I) in NiAlMCM-41 and Ni-AlMCM-41 suggest that Ni(I) is in a framework site in NiAlMCM-41. The differentiation between extraframework and framework sites is confirmed by the effect of sodium ethylenediaminetetraacetate on removing nickel ions from ion-exchanged Ni-AlMCM-41 but not from synthesized NiAlMCM-41.

Introduction

One of the most exciting recent discoveries in the field of porous materials is the formation of mesoporous silica and aluminosilica molecular sieves by using liquid crystal templates. Control of the pore size was achieved to yield solids with molecular sieving properties.[1−4] This family of mesoporous materials, generally called M41S, has large channels from 1.5 to 10 nm ordered in hexagonal (MCM-41), cubic (MCM-48), and lamellar (MCM-50) arrays.[3−7]

The walls of M41S materials seem to be more amorphous than crystalline based on ^{29}Si nuclear magnetic resonance (NMR),[4] and consequently some of the silicons can be substituted by other metals more easily than in crystalline aluminosilicate zeolites.[1] Several transition metals such as vanadium,[8] titanium,[9] zirconium,[10] iron,[11] manganese,[12] and chromium[13] have been stated to be incorporated into the MCM-41 framework. Such materials can be used as catalysts[10,14,15] and heterogeneous hosts for photoionization of bulky organic molecules.[16−18]

Transition metal ions such as Ni(I) or Pd(I) can be active sites for ethylene and propylene dimerization as well as acetylene cyclomerization.[19,20] Several methods have been adopted to introduce Ni(II) ions into molecular sieves followed by reduction to Ni(I) via dehydration in a vacuum at elevated temperatures, thermal reduction in hydrogen, and γ-irradiation at 77 K.[21−24] Dehydration and thermal reduction produce adequate Ni(I) ions in certain materials, but the conditions must be carefully controlled to suppress the formation of metallic nickel clusters. Although γ-irradiation at 77 K produces sufficient Ni(I) ions, other species such as trapped holes on oxygen are also formed during this procedure.[24]

In this study we have hydrothermally synthesized NiMCM-41 and NiAlMCM-41, where Ni(II) is added to the synthesis mixture, and report spectroscopic evidence for nickel ion incorporation into the MCM-41 framework. The formation of Ni(I) in NiAlMCM-41 and its interaction with several adsorbates are compared to Ni(I) formed in ion-exchanged Ni-AlMCM-41 in which Ni(II) is incorporated into extraframework sites.

Experimental Section

Synthesis. The silica sources were aqueous sodium silicate (27 wt % silica, Alfa) and fumed silica (Alfa), the aluminum source was aluminum sulfate (Alfa), the nickel source was nickel nitrate (Mallinckrodt), a 25 wt % aqueous solution of cetyltrimethylammonium chloride (CTAC)(Aldrich) was used as an organic template, and a 25 wt % aqueous solution of tetraethylammonium hydroxide (TEAOH) was obtained from Alfa.

Synthesized Ni-containing siliceous MCM-41 was prepared as follows. Solution 1 was made by adding 9.9 g of TEAOH to 30 g of deionized water with stirring. Solution 2 was prepared by adding the required amount of nickel nitrate in 5 g of deionized water. Then 17.3 g of CTAC followed by 3.0 g of fumed silica was added slowly to solution 1 with stirring for 1 h to form a gel. Solution 2 was then added slowly to this gel and stirred for 1 h. The pH of the mixture was decreased to 11.0 with dilute sulfuric acid. The molar composition of the final gel mixture was SiO_2:0.17 CTACl:0.24 TEAOH:30 H_2O:(0−0.05) Ni. The gels were reacted for 6 days at 373 K in Teflon-lined stainless steel autoclaves. The reaction product was filtered, washed with deionized water, dried in air, and finally calcined in flowing nitrogen while raising the temperature slowly to 813 K and then in flowing air for 10 h. The calcined material was cooled in air and so became hydrated.

The synthesis of Ni-containing AlMCM-41 was performed by a modified method for AlMCM-41 synthesis.[25] A typical

10.1021/jp991035s CCC: $18.00
Published on Web 10/15/1999

synthesis was as follows. A 17.3 g portion of 25 wt % solution of TEAOH was combined with 8.9 g of aqueous sodium silicate dispersed in 75 g of water with stirring. Then 6.8 g of fumed silica and 51.3 g of CTAC solution were added and stirred for 1 h. At the same time, the required amount of aluminum sulfate was dissolved in 5 g of water and slowly added to the silica gel with stirring. The pH of the gel mixture was decreased to 11. 5 by adding dilute sulfuric acid solution and stirred for 1 h. The required amount of nickel nitrate was dissolved in 5 g of deionized water and added to the aluminosilicate gel drop by drop with stirring. Finally, the gel mixture was homogenized for 1 h at room temperature by stirring and then transferred into a Teflon bottle and heated in an oven at 373 K and autogenous pressure for 6 days. The molar composition of the final gel was 1 SiO_2:x Al_2O_3:0.27 CTAC:0.13 Na_2O:0.26 TEAOH:60 H_2O:(0−0.02) Ni, where $x = 0.05$ or 0.025. The solid product was filtered, washed with deionized water several times, and dried in air. The as-synthesized samples were calcined under the same conditions as as-synthesized NiMCM-41 and are termed NiAlMCM-41.

Ni-AlMCM-41, where nickel ions exist in extraframework positions in MCM-41, was prepared by liquid state ion exchange of AlMCM-41(Si/Al =20 in the gel), which was prepared following a literature procedure.[25] AlMCM-41 (0.5 g) was added to 80 mL of 1 mM nickel nitrate solution and stirred for 18 h at room temperature. Finally, the sample was washed with deionized water and filtered.

Sample Treatment and Measurements. The elemental composition of the resultant solid products was analyzed by a JEOL JXA-8600 electron microprobe with a beam diameter of 20 nm. The resolution is 2.5 eV. For the detected elements, the sensitivity is less than 0.03 wt %. Five or more randomly selected spots on the samples were averaged.

The chemical composition of the samples was measured by electron microprobe analysis before and after treatment with an ethylenediaminetetraacetic acid (EDTA)/sodium acetate pH = 5.5 buffer solution.[26] The treatment with EDTA buffer solution was used to remove exchangeable Ni(II) and surface-bound Ni(II) from Ni-containing MCM-41 materials. This was done by stirring 1 g of the sample with 100 mL of 10 mM EDTA buffer solution overnight and then repeating the treatment. The MCM-41 suspension was then filtered and washed.

X-ray powder diffraction patterns were recorded before and after calcination on a Philips PW1840 diffractometer using Cu Kα radiation (40 kV, 25 mA) with a 0.025° step size and 1 s step time over the range $1.2° < 2\theta < 10°$. The samples were prepared as thin layers on aluminum slides.

N_2 adsorption isotherms were measured at 77 K using a Micromeritics Gemini 2375 analyzer. Prior to adsorption, samples were dehydrated at 300 °C for 5 h. The specific surface area, A_{BET}, was determined from the linear part of a BET plot ($P/P_0 = 0.05-0.30$). The pore size distribution was calculated using the adsorption branches of the N_2 adsorption isotherm and the Barret−Joyer−Halenda(BJH) formula.[27]

For ESR measurements, calcined and hydrated samples were loaded into 3 mm o.d. by 2 mm i.d. Suprasil quartz tubes and gradually heated in a vacuum ($<10^{-4}$ Torr) to 373 K and kept at this temperature for 18 h. To study the behavior of the nickel as a function of dehydration, the samples were heated under vacuum from 373 to 773 K at intervals of 100 K. For each interval, the temperature was raised slowly and held at that temperature for 18 h (thermal reduction). Then ESR spectra were measured at 77 K to detect Ni(I) species produced by this thermal reduction. In another reduction method, NiAlMCM-41 and Ni-AlMCM-41 were very slowly heated in a vacuum ($<10^{-4}$ Torr) to 773 K for 12 h and then contacted with 500 Torr of dry oxygen, subsequently heated to 823 K for 5 h, followed by evacuation at 773 K for 1 h to remove oxygen. The samples were then treated with dry hydrogen (50 Torr) at room temperature and subsequently heated to various temperatures from 373 to 723 K for about 30 min (hydrogen reduction). NiMCM-41 was slowly heated in a vacuum ($<10^{-4}$ Torr) to 673 K for 12 h and then contacted with 500 Torr of dry oxygen, subsequently heated to 673 K for 5 h, followed by evacuation at 673 K for 1 h to remove oxygen. The samples were then treated with dry hydrogen (50 Torr) at room temperature and subsequently heated to various temperatures from 373 to 673 K for about 30 min (hydrogen reduction). It should be noted that for the success of these preparations the vacuum line and the hydrogen should be devoid of water since Ni(I) is highly reactive to traces of water.[28] In a third reduction method, calcined samples were loaded into 3 mm o.d. by 2 mm i.d. Suprasil quartz tubes, evacuated at 573 K in a vacuum ($P<10^{-4}$ Torr) for 18 h, and then γ-irradiated at 77 K at a dose rate of 0.2 Mrad/h to a total dose of 1.2 Mrad to reduce some Ni(II) to paramagnetic Ni(I).

TABLE 1: Elemental Composition, Hexagonal Lattice Parameter, a_0, and Surface Area (A) of Calcined Ni-Containing MCM-41

Sample	Si/Al ratio	Si/Ni ratio	a_0 (Å)	A (m^2/g)
Ni-AlMCM-41	15	121	42	1024
NiAlMCM-41	32	80	43	1068
NiMCM-41		130	42	1151

To study interactions with various adsorbates, reduced samples containing Ni(I) were evacuated at room temperature for 10 min and then exposed to the room temperature vapor pressure of D_2O (Aldrich), 100 Torr C_2D_4 (Cambridge Isotope Laboratory), 100 Torr ^{12}CO, and 100 Torr ^{13}CO (Cambridge Isotope Laboratory). These samples with adsorbates were then frozen in liquid nitrogen and sealed. The color of the samples was not changed during these sample treatments. ESR spectra were recorded with a Bruker ESP 300 X-band spectrometer at 77 K. The magnetic field was calibrated with a Varian E-500 gaussmeter. The microwave frequency was measured by a Hewlett-Packard HP 5342A frequency counter. Electron spin−echo modulation (ESEM) spectra were measured at 4 K with a Bruker ESP 380 pulsed ESR spectrometer. Three pulse echoes were measured by using a $\pi/2$-t-$\pi/2$-T-$\pi/2$ pulse sequence as a function of time T to obtain a time domain spectrum. The deuterium modulations were analyzed by a spherical approximation for powder samples in terms of N nuclei at distance R with an isotropic hyperfine coupling A_{iso}.[29] The best fit simulation for an ESEM signal is found by varying the parameters until the sum of the squared residuals is minimized.

Results

Synthesis. The elemental composition and distribution in MCM-41 materials were analyzed by electron microprobe analysis. Table 1 gives the analyzed ratios of Si/Al and Si/Ni for calcined and ion-exchanged samples. Electron microprobe analysis shows that nickel and aluminum are uniformly distributed in these three samples. A highly crystalline sample was only obtained with a low concentration of aluminum (Si/Al > 10) and a low concentration of nickel (Si/Ni > 50).

X-ray Powder Diffraction. Powder XRD patterns of MCM-41 materials taken before and after calcination confirm that the hexagonal MCM-41 phase was formed in these samples (Figures 1 and 2). NiMCM-41 gives a well-resolved XRD pattern, typical

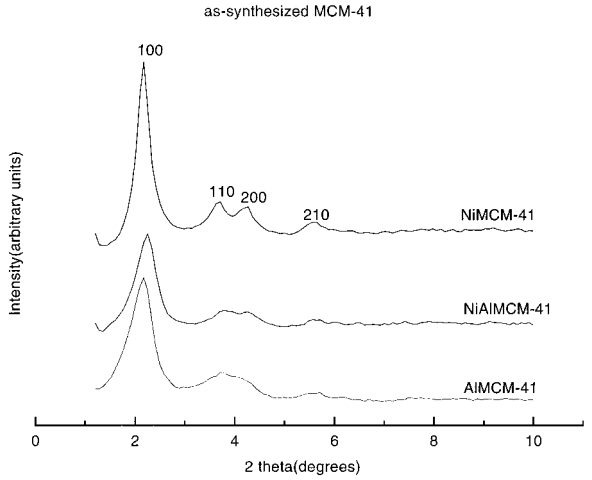

Figure 1. X-ray powder diffraction patterns of as-synthesized NiMCM-41(top), NiAlMCM-41 (middle), and AlMCM-41(bottom).

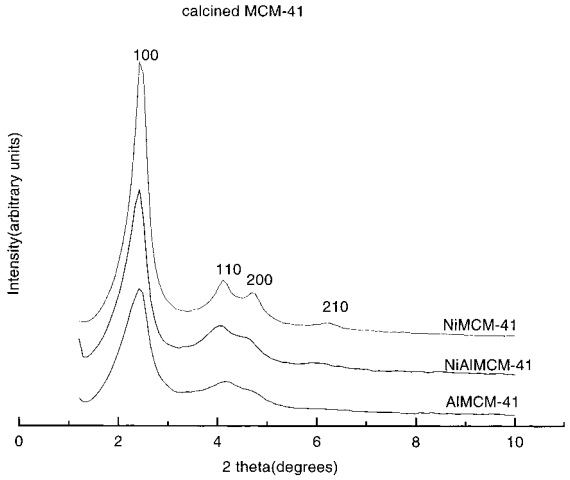

Figure 2. X-ray powder diffraction patterns of calcined NiMCM-41(top), NiAlMCM-41 (middle), and AlMCM-41(bottom).

of MCM-41 material.[4] As-synthesized AlMCM-41 and NiAlMCM-41 give poorer quality XRD patterns with broader peaks than for NiMCM-41. After calcination to remove the surfactant, the XRD pattern of NiAlMCM-41 becomes better resolved (Figure 2). This indicates that atomic rearrangements occur in NiAlMCM-41 when the surfactant molecules are removed.[30]

N_2 Adsorption Isotherms. Low-temperature nitrogen adsorption isotherms enable the measurement of the surface area, pore volume, and mesopore size distribution. The N_2 adsorption isotherm for calcined Ni-containing MCM-41 materials is a type IV adsorption isotherm, typical of mesoporous solids with H_2 hysteresis.[31] At a relative pressure P/P_0 between 0.35 and 0.45, the isotherm exhibits a sharp inflection characteristic of capillary condensation within the mesopores. The sharpness in this step indicates a uniform pore size in these three samples. They have high specific surface areas (Table 1), indicating that they have high crystallinity.

EDTA Treatment. Electron microprobe analysis of NiMCM-41 and NiAlMCM-41 after EDTA treatment indicates that the nickel content is almost unchanged. This suggests that Ni(II) occupies a framework site in these two materials since EDTA complexes Ni(II) strongly and EDTA is expected to remove Ni(II) from surface sites and ion exchange sites.[26] As a check, the treatment of Ni-AlMCM-41 with EDTA buffer solution removes almost all of the nickel ions which are known to be in extraframework ion exchange sites.

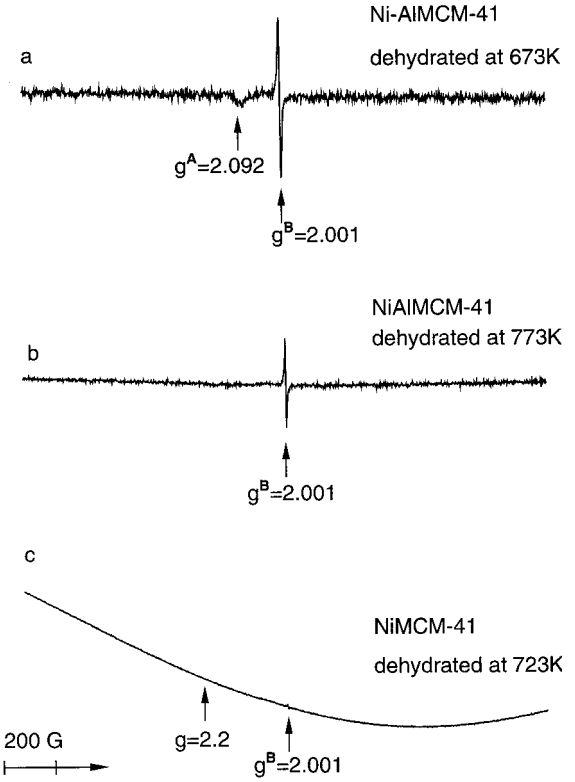

Figure 3. ESR spectra at 77 K of (a) Ni-AlMCM-41 dehydrated at 673 K for 18 h, (b) NiAlMCM-41 dehydrated at 773 K for 18 h, and (c) NiMCM-41 dehydrated at 723 K for 18 h.

Electron Spin Resonance. Calcined and oxidized samples of Ni-containing MCM-41 materials did not show any ESR signal at 77 K consistent with Ni species existing as Ni(II). Figure 3 shows the ESR spectra of Ni-containing MCM-41 materials dehydrated in a vacuum at elevated temperature for 18 h. Dehydration at 673 K leads to the formation of two paramagnetic species, denoted as A and B in Ni-AlMCM-41. Species A can be ascribed to isolated Ni(I) reduced by desorbing water and hydroxyls as suggested earlier.[32] In contrast, NiAlMCM-41 does not show any ESR signal corresponding to species A. Dehydration of this sample even at 723 K does not yield any signal due to Ni(I) species. After thermal reduction, NiMCM-41 shows a broad resonance around $g = 2.2$, which can be assigned to superparamagnetic nickel(0) clusters.[33] Species B is seen in both NiAlMCM-41 and Ni-AlMCM-41. A similar species has also been reported in AlPO and SAPO materials.[21,28] Therefore species B is tentatively assigned to nonspecific framework defects arising due to water or hydroxyl group desorption.

Figure 4 shows the ESR spectra of Ni-containing MCM-41 materials after hydrogen reduction at 723 K. Isolated Ni(I) is observed in Ni-AlMCM-41 and remains after hydrogen outgassing at room temperature. However, for NiAlMCM-41, hydrogen treatment at 723 K does not produce any ESR signals due to isolated Ni(I). For NiMCM-41, hydrogen treatment at 623 K yields superparamagnetic nickel(0) clusters in NiMCM-41, indicating that the reduction of Ni(II) in NiMCM-41 is easier than in Ni-containing AlMCM-41. Conditions were not found where Ni(I) could be stabilized in NiMCM-41.

Isolated Ni(I) ion can be generated in both NiAlMCM-41 and Ni-AlMCM-41 by γ-ray irradiation at 77 K, but no ESR signal ascribable to Ni(I) species is observed in NiMCM-41 after γ-irradiation. This suggests that the stabilization of Ni(I) in NiMCM-41 is minimal. Figure 5 shows ESR spectra at 77

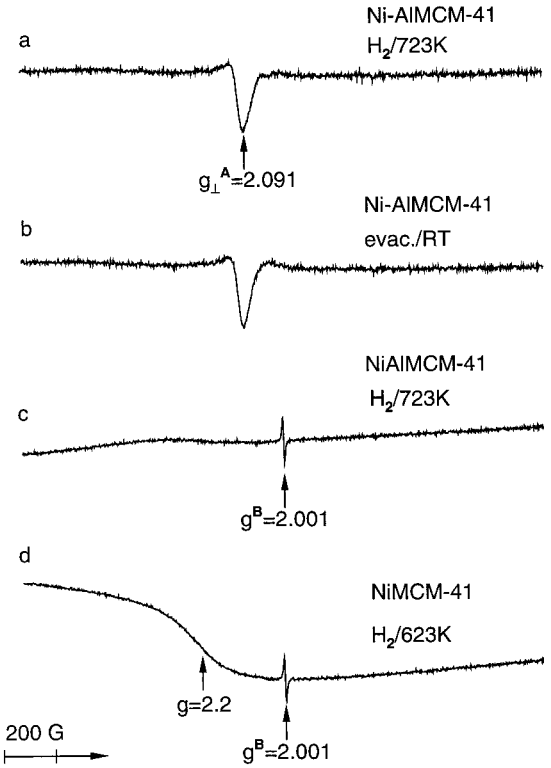

Figure 4. ESR spectra at 77 K of Ni-containing MCM-41 after hydrogen treatment (a) Ni-AlMCM-41 after H_2 treatment at 723 K for 30 min, (b) after 10 min evacuation of (a) at room temperature, (c) NiAlMCM-41 after H_2 treatment at 723 K for 30 min and (d) NiMCM-41 after H_2 treatment at 623 K for 30 min.

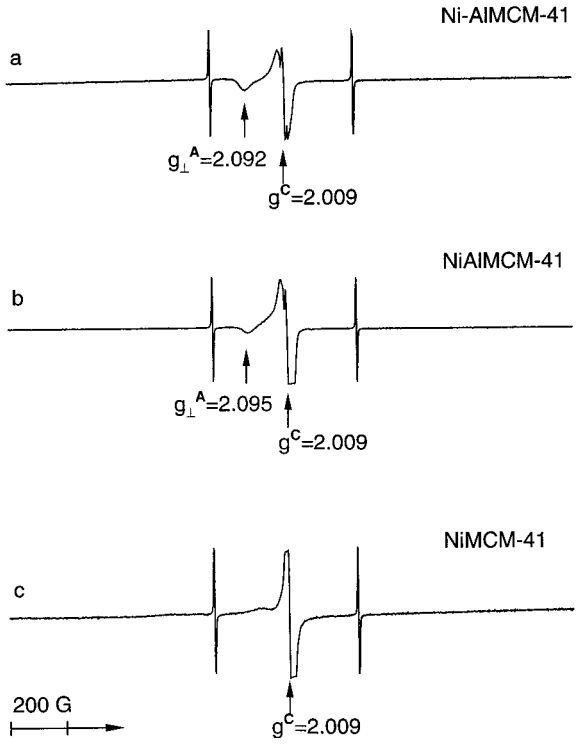

Figure 5. ESR spectra at 77 K of (a) Ni-AlMCM-41, (b) NiAlMCM-41, and (c) NiMCM-41 after γ-irradiation for 6 h.

K after γ-ray irradiation of these three samples. Similar spectra are observed for Ni-AlMCM-41 and NiAlMCM-41. Species A in Ni-AlMCM-41 and NiAlMCM-41 is similar to the species observed by hydrogen reduction of Ni-AlMCM-41 where it is assigned to isolated Ni(I) ions.

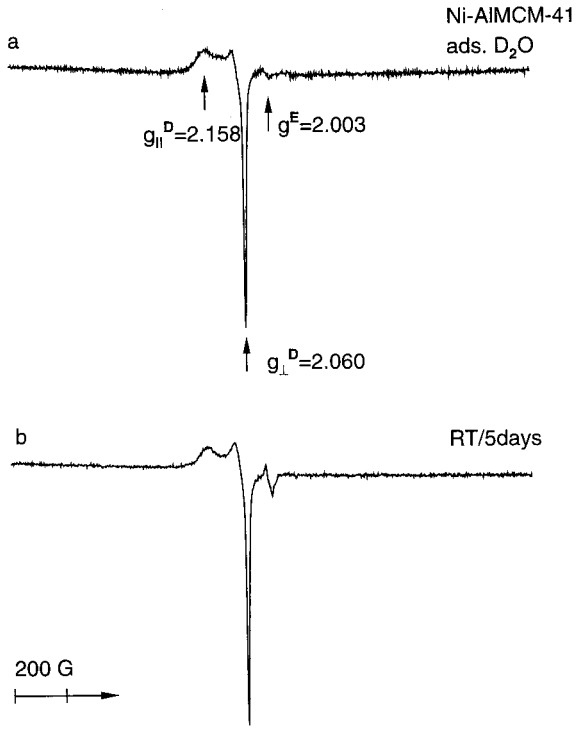

Figure 6. ESR spectra at 77 K of Ni-AlMCM-41: (a) after H_2 reduction at 723 K for 30 min, evacuation at room temperature for 10 min, and subsequent D_2O adsorption for 2 min at room temperature and (b) after annealing (a) at room temperature for 5 days.

Gamma irradiation at 77 K of Y zeolite produces trapped hydrogen atoms (ESR doublet split by 500 G) and trapped holes on oxygen bonded to aluminum or silicon near $g = 2.00$ (V center, species C).[24] These species are similarly assigned here. The ESR signal intensity for species A produced by γ-ray irradiation is substantially higher than the corresponding signal intensity for species A after thermal or hydrogen reduction. The intensity of species A in Ni-AlMCM-41 is higher than in NiAlMCM-41, although the former has lower Ni concentration.

Before adsorbates were added, hydrogen-reduced samples of Ni-AlMCM-41 and γ-ray reduced samples of NiAlMCM-41 were evacuated for 10 min at room temperature. The samples were then exposed to the adsorbates at room temperature for no more than 3 min, because of the instability of Ni(I) at room temperature, and the sample was quenched at 77 K. Figures 6 and 7 show the ESR spectra obtained after D_2O adsorption on Ni-AlMCM-41 and NiAlMCM-41, respectively. D_2O adsorption on Ni-AlMCM-41 and NiAlMCM-41 produces Ni(I) species D with axial symmetry and ESR parameters $g_{\|}^{D} = 2.158$ and $g_{\perp}^{D} = 2.060$. The ESR parameters of species D are almost the same in these two materials. A Ni(I) species with somewhat similar g values and axial symmetry has been reported earlier in Ni-SAPO-34 and assigned to Ni(I)$-(O_2)_n$ produced by the decomposition of water on Ni(I) sites.[34] An ESR signal with similar g values and line shape is observed in Ni-AlMCM-41 and NiAlMCM-41 after adsorption of oxygen. ESEM studies on Ni(I) species D show no deuterium modulation. Thus we assign species D to Ni(I)$-(O_2)_n$.

After D_2O adsorption, Ni(I) species A is destroyed completely in Ni-AlMCM-41, but some remains in NiAlMCM-41 even after annealing at room temperature for 0.5 h. The Ni(I) complex with oxygen (species D) formed after water adsorption on Ni-AlMCM-41 and NiAlMCM-41 is not stable at room temperature, probably because it is oxidized to Ni(II).[32] Figures 6 and 7 show the decay of Ni(I)$-(O_2)_n$ species at room temperature.

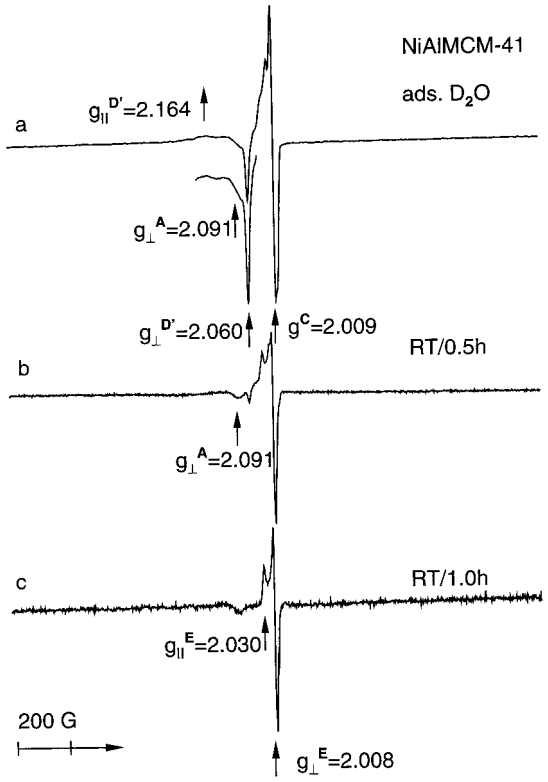

Figure 7. ESR spectra at 77 K of NiAlMCM-41: (a) after γ-ray reduction at 77 K for 6 h, evacuation at room temperature for 10 min, and subsequent D_2O adsorption for 2 min at room temperature, (b) after annealing (a) at room temperature for 0.5 h and (c) after annealing (a) at room temperature for 1 h.

In NiAlMCM-41 the intensitiy of Ni(I)$-(O_2)_n$ decreases rapidly at room temperature and disappears completely after 1 h to form O_2^- radical species E with $g_{||}^{E} = 2.030$ and $g_{\perp}^{E} = 2.008$.[21] This substantiates the oxidation of Ni(I) ion by water. In contrast, in Ni-AlMCM-41 the ESR signal intensity of Ni(I)$-(O_2)_n$ is almost unchanged even after annealing at room temperature for 5 days, but it finally decays without producing observable O_2^- after 13 days. Similar results were previously obtained for NiAPSO-11 versus NiH-SAPO-11.[32] The minor radical species E (Figure 6) at $g = 2.003$ observed after D_2O adsorption on Ni-AlMCM-41 gains intensity upon annealing at room temperature for 5 days and may be assigned to an O_2^- radical. [21]

Adsorption of 100 Torr ^{12}CO on Ni-AlMCM-41 produces Ni(I) species F with rhombic g-tensor components $g_1^F = 2.008$, $g_2^F = 2.117$, and $g_3^F = 2.178$ (Figure 8a). ^{12}CO has a nuclear spin of 0 and therefore shows no hyperfine structure. To identify species F, the same experiment was performed with 99% ^{13}CO. Each of the three g components appears to be split into a quartet with a coupling of 57 G. The observed relative intensity distribution does not completely fit a theoretical one because the g components overlap. Species F is tentatively assigned to Ni(I)$-(CO)_3$. Similar behavior has been reported for CO adsorbed on Ni-SAPO-34 and NiCa-X zeolite.[34,35]

Figure 9a shows the ESR spectrum of NiAlMCM-41 after adsorption of ^{12}CO. A Ni(I) species F′ is observed. After adsorption of 99% ^{13}CO three weak hyperfine peaks with a 24.5 G coupling can be observed on the g_2 component (Figure 9b), showing interaction of two CO molecules with Ni(I). This coordination seems consistent with framework Ni(I) in NiAlMCM-41.

After adsorption of CO, Ni(I) species A in Ni-AlMCM-41 disappears while some remains in NiAlMCM-41. This suggests

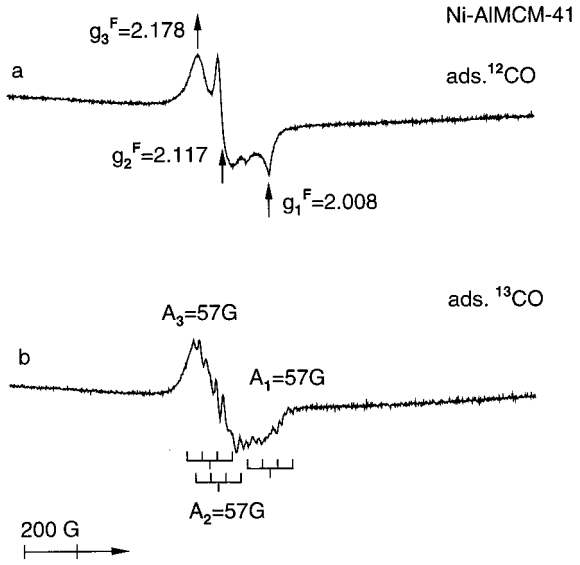

Figure 8. ESR spectra at 77 K of H_2 reduced Ni-AlMCM-41 (a) after ^{12}CO adsorption for 2 min at room temperature and (b) after ^{13}CO adsorption for 2 min at room temperature.

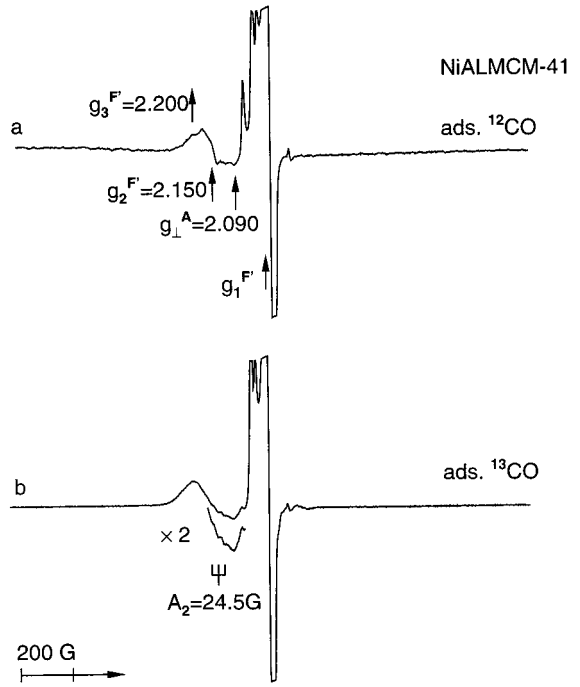

Figure 9. ESR spectra at 77 K of NiAlMCM-41 after γ-ray reduction at 77 K for 6 h, evacuation at room temperature for 10 min (a) ^{12}CO adsorption for 2 min at room temperature and (b) after ^{13}CO adsorption for 2 min at room temperature.

that some Ni(I) in NiAlMCM-41 is less accessible to CO than in Ni-AlMCM-41.

A new Ni(I)$-C_2D_4$ complex is formed in Ni-AlMCM-41 after 2 min exposure to ethylene (Figure 10a). This is supported by ESEM data.[23] After annealing at room temperature for 0.5 h, the Ni(I)$-C_2D_4$ complex almost disappears and a new Ni(I) species I with $g_{||}^{I} = 2.051$ and $g_{\perp}^{I} = 2.030$ is formed (Figure 10b). Species I is also obtained after *n*-butene adsorption on Ni-AlMCM-41. ESEM analysis of the deuterium modulation of species I shows interaction of eight deuteriums with one Ni(I), indicating butene formation (Figure 11). Another Ni(I) species G is perhaps due to Ni(I) coordination with traces of water introduced during exposure to ethylene.[28] Species G seems to be the same as species D formed during D_2O adsorption.

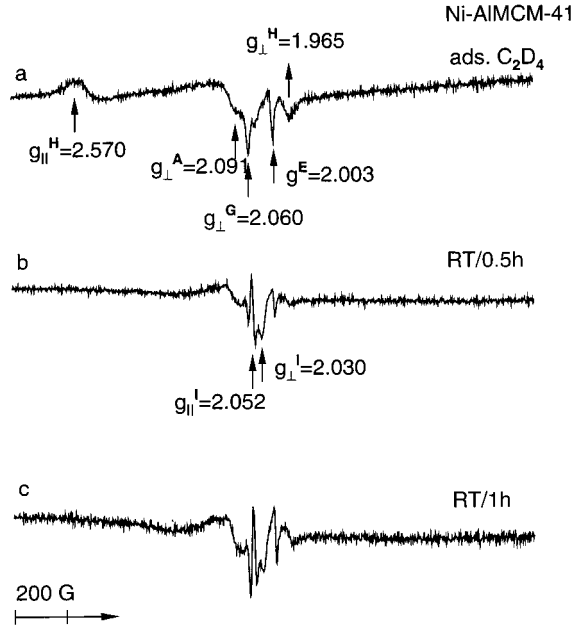

Figure 10. ESR spectra at 77 K of Ni-AlMCM-41 (a) after hydrogen reduction, evacuation at room temperature for 10 min, and subsequent C_2D_4 adsorption for 2 min at room temperature, (b) after annealing (a) at room temperature for 0.5 h, and (c) after annealing (a) at room temperature for 1 h.

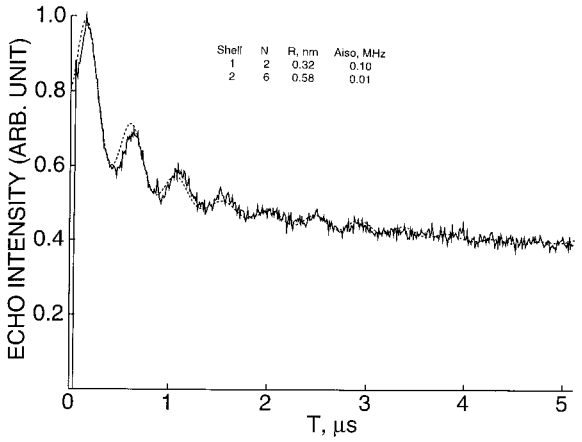

Figure 11. Experimental (−) and simulated (- - -) three pulse ESEM spectrum at 4.2 K and $g = 2.052$ showing D modulation in Ni-AlMCM-41 with adsorbed C_2D_4 after annealing at room temperature for 0.5 h.

On the other hand, C_2D_4 exposure to NiAlMCM-41 for 2 min at room temperature yields only a weak rhombic species J, which is assigned to the Ni(I)−C_2H_4 complex (Figure 12 a).[32] After annealing at room temperature for 1 h, most Ni(I) ions still remain and no new species is formed. ESEM studies for species J show no deuterium modulation.

Table 2 summarizes the ESR parameters assigned to the various Ni(I) species observed in NiAlMCM-41 and Ni-AlMCM-41.

Discussion

NiMCM-41, NiAlMCM-41, and AlMCM-41 have good crystallinity and high surface area. The XRD peaks of NiMCM-41 for the 110, 200, and 210 reflections are reasonably well resolved. The less resolved XRD peaks for NiAlMCM-41 and AlMCM-41 may be due to the formation of smaller crystallites.[2]

Ni(I) ions formed by reduction of Ni(II) can be stabilized in zeolites[22] and SAPO materials.[21,28] The reducibility of Ni(II) in zeolites and other molecular sieves depends on the structure

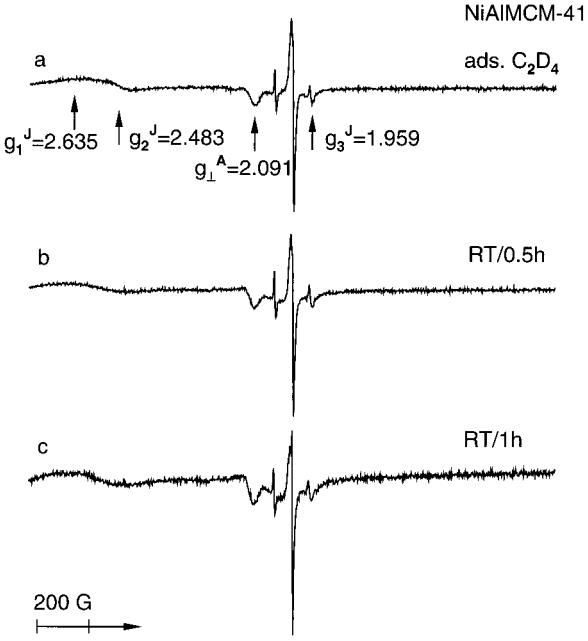

Figure 12. ESR spectra at 77 K of NiAlMCM-41 (a) after γ-ray reduction, evacuation at room temperature for 10 min, and subsequent C_2D_4 adsorption for 2 min at room temperature, (b) after annealing (a) at room temperature for 0.5 h, and (c) after annealing (a) at room temperature for 1 h.

type and the ion concentration and location.[36] The reducibility of Ni(II) in Y zeolite,[36] SAPO-41,[21] and hydroxyhectorite clay materials[26] has been studied previously. The location of the cation site and its access to reducing agents controls the reduction efficiency.

Synthesized NiAlMCM-41 and ion-exchanged Ni-AlMCM-41 differ considerably in their behavior toward dehydration at elevated temperature. Ni-AlMCM-41 produces Ni(I) when dehydrated at temperatures above 573 K as observed by ESR (Figure 3). Water or hydroxyl groups are suggested to be responsible for this reduction. Kasai et al. suggested that the reduction of Cu(II) ions in Cu(II)-exchanged modenite zeolite that occurs upon heating in a vacuum is due to reduction by residual water.[37] Michalik et al. suggested that water in PdCa-X zeolite plays a role in the reduction of Pd(II) upon heating in a vacuum.[38]

In contrast, NiAlMCM-41 does not yield any ESR signal of Ni(I) when dehydrated even at 773 K. This difference between NiAlMCM-41 and Ni-AlMCM-41 is also found by heating in the presence of hydrogen at moderate to high temperatures. An isolated Ni(I) species with axially symmetric g values is formed when Ni-AlMCM-41 is reduced at 673 K. On the other hand, similar hydrogen treatment on NiAlMCM-41 is ineffective in producing Ni(I) and no ESR signal of Ni(I) is seen. Similar results were obtained from Ni(II)-substituted SAPO-41 versus Ni(II)-exchanged SAPO-41.[21] The fact that both NiAlMCM-41 and Ni-AlMCM-41 behave differently on dehydration and hydrogen treatment suggests that Ni(II) in NiAlMCM-41 is in a different site than in Ni-AlMCM-41.

Although thermal and hydrogen reduction are ineffective for producing Ni(I) in NiAlMCM-41, γ-irradiation at 77 K is effective as shown by ESR (Figure 5). This suggests that Ni(II) in NiAlMCM-41 is in a more stable site than in Ni-AlMCM-41. Similar results were reported for Ni(II)-substituted and ion-exchanged SAPO-41 and hydroxyhectorite clay materials.[21,26]

The behavior of NiAlMCM-41 and Ni-AlMCM-41 after adsorbing D_2O, CO, and C_2D_4 also shows some differences

TABLE 2: ESR *g* Values of Ni(I) Species in NiAlMCM-41 and Ni-AlMCM-41 after Various Reduction Methods and after Adsorbate Addition

reduction method	sample	adsorbate	species	assignment	$g_{\|\|}$ or g_1	$g_\perp$ or g_2	g_3
thermal	NiAlMCM-41						
	Ni-AlMCM-41		A	Ni(I)	*a*	2.092	
H_2	NiAlMCM-41						
	Ni-AlMCM-41		A	Ni(I)	*a*	2.091	
γ-ray	NiAlMCM-41		A	Ni(I)	*a*	2.095	
	Ni-AlMCM-41		A	Ni(I)	*a*	2.092	
γ-ray	NiAlMCM-41	D_2O	D′	Ni(I)$-(O_2)_n$	2.158	2.060	
H_2	Ni-AlMCM-41	D_2O	D	Ni(I)$-(O_2)_n$	2.158	2.060	
γ-ray	NiAlMCM-41	CO	F′	Ni(I)$-(CO)_2$	*b*	2.150	2.200
H_2	Ni-AlMCM-41	CO	F	Ni(I)$-(CO)_3$	2.008	2.117	2.178
γ-ray	NiAlMCM-41	C_2D_4	J	Ni(I)$-(C_2D_4)_n$	1.959	2.483	2.635
H_2	Ni-AlMCM-41	C_2D_4	H	Ni(I)$-C_2D_4$	2.570	1.965	
			I	Ni(I)$-C_4D_8$	2.052	2.030	

[a] The $g_{\|\|}$ peak is too weak to be observed. [b] The g_1 peak overlaps with the ESR signal of a V center.

which can be attributed to a difference in Ni(I) locations. After D_2O adsorption, Ni(I) species A in Ni-AlMCM-41 interacts with D_2O to produce a more stable Ni(I) species D. However, only part of the Ni(I) in NiAlMCM-41 interacts with D_2O even after annealing at room temperature for 0.5 h, and species D′ vanishes after annealing at room temperature for 1 h and transforms to Ni(II)$-O_2^-$.[21] The lack of interaction of all Ni(I) with D_2O is consistent with part of the nickel ions being located inside the hexagonal tubular walls of NiAlMCM-41 because Ni(I) is highly reactive to water.

There are also some differences between the Ni(I) parameters in NiAlMCM-41 and Ni-AlMCM-41 after CO adsorption. ^{13}CO adsorption of Ni-AlMCM-41 produces four hyperfine lines, indicating Ni(I)$-(CO)_3$ formation, and Ni(I) species A vanishes. In contrast, for NiAlMCM-41 ^{13}CO adsorption produces three weak hyperfine lines on the g_2 component indicating Ni(I)$-(CO)_2$ formation. Some Ni(I) remains after CO adsorption on NiAlMCM-41, indicating that some Ni(I) is less accessible in NiAlMCM-41 than in Ni-AlMCM-41.

Ethylene adsorption shows other significant evidence for a Ni(II) location difference between NiAlMCM-41 and Ni-AlMCM-41. A Ni(I)$-C_2D_4$ complex is formed in Ni-AlMCM-41 after 2 min exposure to ethylene. A new Ni(I)$-C_4D_8$ complex is produced after annealing at room temperature for 0.5 h, indicating that Ni(I) in Ni-AlMCM-41 has high ethylene dimerization activity. On the other hand, C_2D_4 exposure to NiAlMCM-41 for 2 min at room temperature yields only very weak Ni(I) species J. No new species is formed after annealing at room temperature for 1 h, and most of the Ni(I) ions remain. ESEM studies for species J show no deuterium modulation, suggesting that the distance between deuterium and Ni(I) in NiAlMCM-41 is too large to produce deuterium modulation. When ethylene is adsorbed onto Ni(I) in NiCa$-$X and Ni$-$CaY, extraframework Ni(I) disappears rapidly with formation of a Ni(I)$-$ethylene complex within 30 min.[39,40] Thus, the interaction of Ni(I) in NiAlMCM-41 with C_2D_4 seems weaker than that of Ni(I) in Ni-AlMCM-41, NiCa$-$X, and NiCa$-$Y with C_2D_4. This indicates that most of the nickel ions are in a less accessible site in NiAlMCM-41 than in Ni-AlMCM-41.

A difference in the location of nickel ions between NiAlMCM-41 and Ni-AlMCM-41 is also supported by electron microprobe analysis before and after EDTA treatment. The nickel concentration in NiAlMCM-41 is almost unchanged after EDTA treatment. In contrast, almost all of the nickel ions are removed by EDTA treatment from Ni-AlMCM-41 in which nickel ions are in extraframework sites. These results indicate that the nickel ion in NiAlMCM-41 is incorporated into a framework site. Similar results were obtained for Ni(II)-substituted synthetic hydroxyhectorites versus Ni(II)-exchanged hydroxyhectorites.[26]

Overall, the data seem clear that the nickel ion sites in NiAlMCM-41 and in Ni-AlMCM-41 are quite different. Since nickel ion is clearly in a nonframework site in Ni-AlMCM-41, these results seem to support the assignment of nickel ions in NiAlMCM-41 to a framework site.

Conclusions

Hydrothermal synthesis of NiAlMCM-41 and NiMCM-41 mesoporous molecular sieves has been achieved using cetyltrimethylammonium chloride as the template. Stabilization of Ni(I) in NiMCM-41 is minimal. However, Ni(I) species can be stabilized in NiAlMCM-41 and Ni-AlMCM-41. Comparative ESR and ESEM studies between synthesized NiAlMCM-41 and ion-exchanged Ni-AlMCM-41 show significant differences with respect to nickel ion reduction, location and adsorbate interaction. Thermal and hydrogen reduction produce Ni(I) ions in Ni-AlMCM-41; however, these methods are not effective in NiAlMCM-41. Although thermal and hydrogen reduction do not produce Ni(I) species in NiAlMCM-41, γ-irradiation does produce Ni(I) suggesting that Ni(II) is more stable in NiAlMCM-41 than in Ni-AlMCM-41. Both NiAlMCM-41 and Ni-AlMCM-41 show differences in their ESR spectra after D_2O, CO, and C_2D_4 adsorption at room temperature. Upon adsorbing D_2O, Ni(I)$-(O_2)_n$ complex is formed in both materials and is more stable in Ni-AlMCM-41 than in NiAlMCM-41. Analysis of the ^{13}CO hyperfine after ^{13}CO adsorption shows a Ni(I)$-(CO)_3$ species in Ni-AlMCM-41 and a Ni(I)$-(CO)_2$ species in NiAlMCM-41. Ethylene dimerizes to form butene on activated Ni-AlMCM-41, but the interaction of ethylene with Ni(I) in NiAlMCM-41 is weak. The contrasting coordination properties of Ni(I) indicate that its local environment in synthesized NiAlMCM-41 is different from that in ion-exchanged Ni-AlMCM-41. The cation location difference is confirmed by the effect of EDTA on removing Ni(II) from ion-exchanged Ni-AlMCM-41 but not from synthesized NiAlMCM-41. Since Ni(II) in Ni-AlMCM-41 is clearly in a nonframework site, these results support that Ni(II) in synthesized NiAlMCM-41 is in a framework site.

Acknowledgment. This research was supported by the National Science Foundation, the Robert A. Welch Foundation, and the University of Houston Energy Laboratory.

References and Notes

(1) Vartuli, J. C.; Shih, S. S.; Kresge, C. T.; Beck, J. S. In *Mesoporous Molecular Sieves*; Bonneviot, L., Beland, F., Danumah, C., Giasson, S.,

Kaliaguine, S., Eds.; Studies in Surface Science and Catalysis, Vol. 117; Elsevier: Amsterdam, 1998; p 13.
(2) Corma, A. *Chem. Rev.* **1997**, *97*, 273.
(3) Kresge, C. T.; Leonowicz, M. E.; Roth, W. J.; Vartulli, J. C.; Beck, J. S. *Nature* **1992**, *359*, 710.
(4) Beck, J. S.; Vartuli, J. C.; Roth, W. J.; Leonowicz, M. E.; Kresge, C. T.; Schmitt, K. D.; Chu, C. T.−W.; Olson, D. H.; Sheppard, E. W.; McCullen, S. B.; Higgins, J. B.; Schlenker, J. L. *J. Am. Chem. Soc.* **1992**, *114*, 10834.
(5) Vartuli, J. C.; Kresge, C. T.; Leonowicz, M. E.; Chu, A. S.; McCullen, S. B.; Johnson, I. D.; Sheppard, E. W. *Chem. Mater.* **1994**, *6*, 2070.
(6) Beck, J. S.; Vartuli, J. S.; Kennedy, G. J.; Kresge, C. T.; Roth, W. J.; Schramm, S. E. *Chem. Mater.* **1994**, *6*, 2070.
(7) Vartuli, J. C.; Schmitt, K. D.; Kresge, C. T.; Roth, W. J.; Leonowicz, M. E.; McCullen, S. B.; Hellring, S. D.; Beck, J. S.; Schlenker, J. L.; Olson, D. H.; Sheppard, E. W. In *Zeolites and Related Microporous Materials*; Weitkamp, J., Karge, H. G., Pfeifer, H., Holderich, W., Eds.; Studies in Surface Science and Catalysis, Vol. 84; Elsevier: Amsterdam, 1994; p 53.
(8) Luan, Z.; Xu, J.; He, H.; Klinowski, J.; Kevan, L. *J. Phys. Chem.* **1996**, *100*, 19595.
(9) Corma, A.; Navarro, M. T.; Perez-Pariente, J. *J. Chem. Soc., Chem. Commun.* **1994**, 147.
(10) Gontier, S.; Tuel, A. *Applied Catalysis A: General* **1996**, *143*, 125.
(11) Yuan, Z. Y.; Liu, S. Q.; Chen, T. H.; Wang, J. Z.; Li, H. X. *J. Chem. Soc., Chem. Commun.* **1995**, 973.
(12) Xu, J.; Luan, Z.; Wasowicz, T.; Kevan, L. *Micro. Meso. Mater.* **1998**, *22*, 179.
(13) Zhang, W.; Pinnavaia, T. J. *Catal. Lett.* **1996**, *38*, 261.
(14) Corma, A.; Grande, M. S.; Gonzalez-Alfaro, V.; Orchilles, A. V. *J. Catal.* **1996**, 159, 375.
(15) Hartmann, M.; Poppl, A.; Kevan, L. *J. Phys. Chem.* **1996**, *100*, 9906.
(16) Corma, A.; Fornes, V.; Carcia, H.; Miranda, M. A.; Sabater, A. *J. Am. Chem. Soc.* **1994**, *98*, 1253.
(17) Sung-Sub, H. M.; Luan, Z.; Kevan, L. *J. Phys. Chem.* **1997**, *101*, 10455.
(18) Cano, M. L.; Cozens, T-. L.; Garcia, H.; Marti, V.; Sciano, J. C. *J. Phys. Chem.* **1996**, *100*, 18152.
(19) Kazansky, V. B.; Elev, I. V.; Shelimov, B. N. *J. Mol. Catal.* **1983**, *21*, 265.
(20) Bonneviot, L.; Olivier, D.; Che, M. *J. Mol. Catal.* **1983**, *21*, 415.
(21) Prakash, A. M.; Hartmann, M.; Kevan, L. *J. Chem. Soc., Faraday Trans.* **1997**, *93*, 1233.
(22) Michalik, J.; Narayana, M.; Kevan, L. *J. Phys. Chem.* **1984**, *88*, 5236.
(23) Hartmann, M.; Poppl, A.; Kevan, L. *J. Phys. Chem.* **1996**, *100*, 9906.
(24) Abou-Kais, A.; Vedrine, J. C.; Massardier, J.; Dalmai-Imelik, G. *J. Chem. Soc., Faraday Trans. 1* **1974**, *70*, 1039.
(25) Luan, Z.; Cheng, C.; Zhou W.; Klinowski, J. *J. Phys. Chem.* **1995**, *99*, 1018.
(26) Yamada, H.; Azuma, N.; Kevan, L. *J. Phys. Chem.* **1994**, *98*, 13107.
(27) Barret, E. P.; Joyner, L. G.; Halenda, P. P. *J. Am. Chem. Soc.* **1951**, *73*, 373.
(28) Azuma, N.; Hartmann, M.; Kevan, L. *J. Phys. Chem.* **1995**, *99*, 6670.
(29) Kevan, L. In *Time Domain Electron Spin Resonance*; Kevan, L., Schwartz, R. N., Eds.; Wiley: New York, 1979; Chapter 8.
(30) Luan, Z.; Xu, J.; He, H.; Klinowski J.; Kevan, L. *J. Phys. Chem.* **1996**, *100*, 19595.
(31) Sing, K. S. W.; Everett, D. H.; Haul, R. A. W.; Mosco, L.; Pierott, R. A.; Rouquerol, J.; Siemieniewska, T. *Pure Appl. Chem.* **1985**, *57*, 603.
(32) Azuma, N.; Lee, C. W.; Kevan, L. *J. Phys. Chem.* **1994**, *98*, 1217.
(33) Che, M.; Richard, M.; Olivier, D. *J. Chem. Soc., Faraday Trans. 1* **1980**, *79*, 526.
(34) Djieugoue, M.; Prakash, A. M.; Kevan, L. *J. Phys. Chem.* **1998**, *102*, 4386.
(35) Kermarec, M.; Olivier, D.; Richard, M.; Che, M. *J. Phys. Chem.* **1982**, *86*, 2818.
(36) Schoonheydt, R. A.; Roodhooft, D. *J. Phys. Chem.* **1986**, *90*, 6319.
(37) Kasai, P. H.; Bishop, R. J., Jr. *J. Phys. Chem.* **1977**, *81*, 1527.
(38) Michalik, J.; Narayana, M.; Kevan, L. *J. Phys. Chem.* **1985**, *89*, 4553.
(39) Ghosh, A. K.; Kevan, L. *J. Phys. Chem.* **1990**, *94*, 3117.
(40) Michalik, J.; Narayana, M.; Kevan, L. *J. Phys. Chem.* **1984**, *88*, 5236.